Journal of Global Positioning Systems (2010)
Vol.9, No.1: 61-67
DOI: 10.5081/jgps.9.1.61

Journal of Global Positioning Systems
2010
© CPGPS

Magnitudes and Temporal Variations of the Tropospheric and Ionospheric Errors in GPSnet

Suqin Wu, Kefei Zhang, David Silcock
School of Mathematics and Geospatial Science, RMIT University, Australia

Abstract

One of the main factors that lead to better performance of a Network RTK (NRTK) system is to predict/generate and transmit high accuracy error corrections from the central server for the rover's location without much latency. The corrections are mainly for the atmospheric errors i.e. the tropospheric and ionospheric errors. These two types of atmospheric errors can be calculated and transmitted either separately or together, depending on the way the NRTK system is implemented. It is commonly thought that the magnitudes and temporal variations of the two types of atmospheric errors are quite different. For example, it is often emphasized that the ionospheric errors vary more quickly with time and so more difficult to be modeled than the tropospheric errors.

In this paper, comparisons of the differences in the magnitudes and temporal variations between the double differenced (DD) tropospheric and ionospheric errors were conducted using GPS observations from GPS*net*, the Victorian CORS network. Test results indicated that both types of the DD atmospheric errors significantly contaminate GPS measurements regardless whether it was day time or nighttime. Test results also showed that the temporal variation amplitudes of the DD tropospheric residuals in a fixed time span was not always significantly less than that of ionospheric residuals. In some cases, the DD tropospheric residuals reached several centimetres in a one-minute time span. These results can be instructive in the determination of the way a NRTK system is implemented, e.g. the rates or frequencies for generating and transmitting both types of atmospheric corrections.

Keywords: NRTK, GPS*net*, tropospheric errors, ionospheric errors, atmospheric errors.

1. Introduction

The overall performance of a NRTK system depends on several factors such as the accuracy of interpolated error corrections for the rover's locations, the frequencies for the correction generation and transmission, and the latency of the correction data etc. The interpolated error corrections are usually derived from a real-time regional error model, which is derived from the GPS reference station networks. The regional error models as well as the interpolated corrections for the rover's locations are mainly for the spatially correlated errors (also called distance-dependent errors). These types of errors consist of the satellite orbital errors and the atmospheric errors. If the ground GPS baselines are short e.g. less than 10 km, and the double differencing approach is used in the data processing, like the case of most NRTK approaches, then the most part of the spatially correlated errors can be cancelled out in the baseline's DD observation equations. For the medium length of baselines (e.g. 10−100 km), if precise GPS orbit products such as IGS precise orbits (IGSCB, 2009) are used, the effect of the orbital errors on the baseline length will be at a few mm level (Wu, 2009), which is insignificant and so negligible for the cm level accuracy of NRTK positioning. In this case, the remained errors to be modeled mainly contain the atmospheric errors.

The troposphere and ionosphere, as the two components of the atmosphere, both are located in different height ranges or layers above the earth's surface. Their effects on GPS measurements, so-called the tropospheric and ionospheric errors/delays, are both spatially and temporally correlated. The approach of multiple reference station networks, especially for NTRK is just based on these natures. For example, the regional error modeling as well as error interpolation is based on the characteristic of spatially correlation, whereas the error predictions for the rover's location for the future's epochs is based on the characteristic of temporal variation.

For GPS multiple reference station approaches, over the past years, more attentions have been attracted to the study of the ionospheric errors. Many researchers kept emphasizing that the ionospheric errors vary with time quicker than the tropospheric errors, especially in the solar maximum periods. Hence it is more difficult to

predict the ionospheric errors accurately, compared to the tropospheric errors. These may be true in many cases and especially for undifferenced (one-way) GPS observations. However in the case of differential GPS approaches, e.g. the DD approach that is mostly used in NRTK systems, the temporal variations of DD ionospheric and tropospheric errors may not be as straightforward as that of the undifferenced case. This is because the DD errors derived from four one-way observables. The magnitudes and variations of the DD tropospheric and ionospheric errors are mainly related to the geometry formed by the two associated stations and two satellites. Therefore, the characteristics e.g. the magnitudes and temporal variations of the atmospheric errors can be quite different between the undifferenced and DD cases. Theoretically, it is difficult to justify, between the two types of atmospheric errors for the DD case, if it is true that the magnitudes and temporal variations of the DD tropospheric errors are still generally much smaller than that of the DD ionospheric errors. Tests with real observations are necessary for the region of interest. In this paper, tests using GPS observations from GPS*net* with different baselines and different observation sessions were conducted. The methodology, test results, and conclusions will be elaborated in the following sections.

2. Methodology

The double differenced carrier phase observation equations on either L1 or L2 can be expressed as (Hofmann-Wellenhof et al., 1997)

$$\lambda_k \nabla\Delta\phi_k = \nabla\Delta\rho + \lambda_k \nabla\Delta N_k + \nabla\Delta T - \alpha_k \nabla\Delta I + \varepsilon_{(\nabla\Delta\phi_k)} \quad (1)$$

Where k=1 or 2; T and I denote the tropospheric and ionospheric residuals respectively; the subscript k denotes either of the two frequencies of L1 and L2;
And

$$\alpha_1 = \frac{f_2^2}{f_1^2 - f_2^2} \quad (2)$$

$$\alpha_1 = \frac{f_1^2}{f_1^2 - f_2^2} \quad (3)$$

From the Geometry-free (GF) combination of the two GPS carrier phase observables on L1 and L2 expressed in equation (1), neglecting the last term for the random errors at the right-hand side of equations (1), the DD ionospheric residual on L1 for a baseline and a satellite pair can be obtained from either of the following two expressions:

$$\nabla\Delta I_{L1} = (-\frac{f_2^2}{f_1^2 - f_2^2}) \cdot [(\lambda_1 \nabla\Delta\phi_1 - \lambda_2 \nabla\Delta\phi_2) - (\lambda_1 \nabla\Delta N_1 - \lambda_2 \nabla\Delta N_2)] \quad (4)$$

If the ambiguity for widelane, rather than for $\nabla\Delta N_2$, is resolved, the following expression may be used:

$$\nabla\Delta I_{L1} = (-\frac{f_2^2}{f_1^2 - f_2^2}) \cdot [\nabla\Delta\phi_1 (\frac{c}{f_1} - \frac{c}{f_2}) + \nabla\Delta\phi_w \cdot \frac{c}{f_2} - \nabla\Delta N_1 (\frac{c}{f_1} - \frac{c}{f_2}) - \nabla\Delta N_w \cdot \frac{c}{f_2}] \quad (5)$$

Where the subscript of *w* denotes widelane.

Similarly, from an ionosphere-free (IF) combination (e.g. (77,−60)), the DD tropospheric residual can be calculated by:

$$\nabla\Delta T = \lambda_{77,-60} \nabla\Delta\phi_{77,-60} - \nabla\Delta\rho - (17\lambda_{77,-60}) \nabla\Delta N_1 - (60\lambda_{77,-60}) \nabla\Delta N_w \quad (6)$$

After the DD ambiguities for a baseline and a satellite pair are resolved, the DD ionospheric and tropospheric residuals for the baseline and the satellite pair can be estimated from the above formulae on an epoch-by-epoch and a satellite-by-satellite basis.

In this research, for the network ambiguity resolution, the widelane ambiguities are resolved first, then conventional Kalman filter is used to resolve the L1 ambiguities $\nabla\Delta N_1$, and the IF combination (77,−60) is used as the measurement equation in the Kalman filter. The details of the algorithms used in this procedure and all of the notations used in equations (5) and (6) can be found in (Chen *et al.*, 2000; Wu, 2009).

3. Test Data

The test data is from GPS*net*, the regional GPS Continuously Operating Reference Station (CORS) network in the state of Victoria, Australia. Currently GPS*net* consists of 33 reference stations covering both the Melbourne metropolitan and rural areas of Victoria. The inter-station distances of GPS*net* range from several tens of kilometres up to 200km, a typical medium-to-long-range GPS reference network. More details of GPS*net* can be found from (SII, 2008).

Three baselines from the GPS*net* sites were selected for tests. The names, lengths and stations of the three selected baselines are shown in Fig. 1. GPS data from three different observation sessions is also used for the tests. The three observation sessions and sampling rates of the data are listed in Table 1. Sessions A, B and C are for the tests of Baseline-A, Baseline-B and Baseline-C of Fig. 1 respectively. The test results are presented in the following sections.

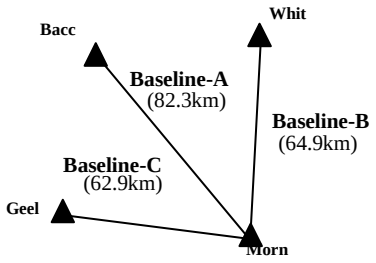

Figure 1: Test baselines from GPS*net*.

Table 1: Three observation sessions

Session names	Observation periods (local)	Sampling rates
A	1:30pm−2:30am, 13−14/11/2007	30s
B	7am−11am, 26/07/2008	5s
C	12pm−4pm, 01/06/2007	10s

4. Test Results

4.1 Magnitudes

a) Baseline-A

Using formulae (5) and (6), both DD tropospheric and ionospheric errors/residuals for Baseline-A, observations of Session A, and for each of the satellite pairs are calculated. Figs 2a and 2b show the time series plots for the test results of the six selected satellite pairs. The statistical values (RMS) for the results of the time series are listed in Table 2. It should be noted that the word "satellite" used in all of the figures actually means "satellite pair". However, the reference satellites are not shown there since they vary with time. The system automatically selects the one with the highest elevation at an epoch to be the reference satellite of the epoch for the double differencing used by other satellites.

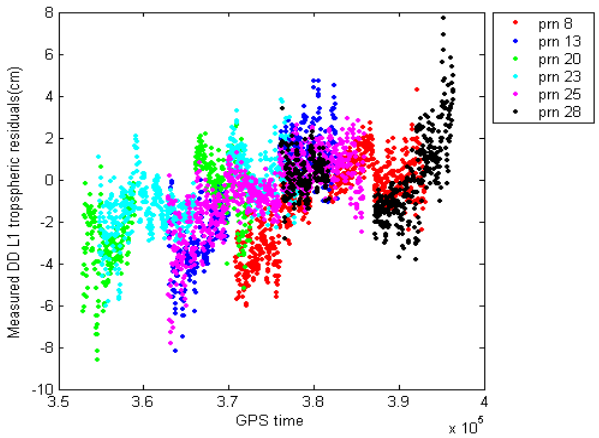

Figure 2a: Time series plots for the measured DD L1 tropospheric residuals of Baseline-A and six satellites; 13-hour data from Session A is used.

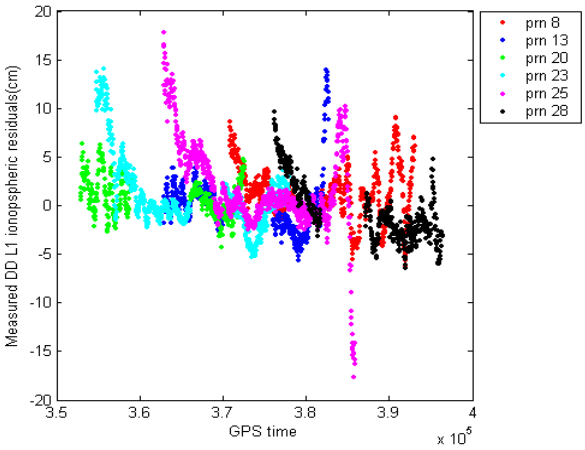

Figure 2b: Time series plots for the measured DD L1 ionospheric residuals of Baseline-A and six satellites; 13-hour data from Session A is used.

Table 2: RMS (cm) values for the measured DD L1 tropospheric and ionospheric residuals of Baseline-A and six satellites.

PRN	8	13	20	23	25	28
Trop.	2.1	2.8	2.6	1.7	1.8	3.3
Iono.	2.9	3.1	2.1	4.0	4.9	3.1

Note: the shaded/yellow areas mean that the RMS value of the tropospheric residuals is greater than that of the ionospheric residuals for the same satellite.

From Figs 2a and 2b, and Table 2, we can see:

1. The maximum values of the DD tropospheric and ionospheric residuals are about 8 cm and 18 cm respectively.
2. The majority of the RMS values of the DD tropospheric residuals are less than that of the ionospheric residuals.

b) Baseline-B

Figs 3a and 3b show the time series plots for the results of Baseline-B and six satellites. The test data from Session B is used. Table 3 shows the statistical values (RMS) for the results of the time series.

From Figs 3a and 3b, and Table 3, it can be seen:

1. The maximum values of the DD tropospheric and ionospheric residuals are about 13 cm and 8 cm respectively.
2. Out of the six satellites, five satellites' RMS values of the DD tropospheric residuals are greater than that of the ionospheric residuals.
3. The results of Baseline-B are quite different from that of Baseline-A.

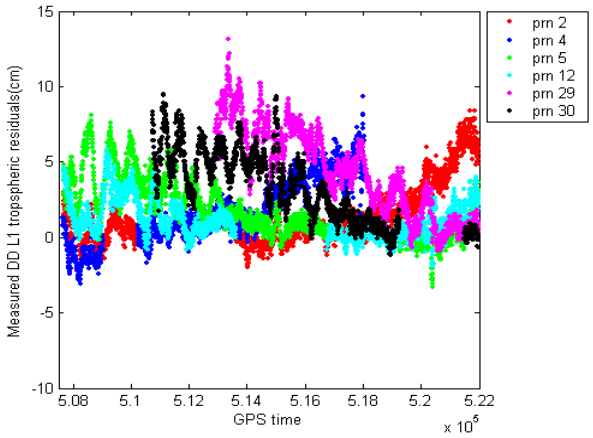

Figure 3a: Time series plots for the measured DD L1 tropospheric residuals of Baseline-B and six satellites, 4-hour data from Session B is used.

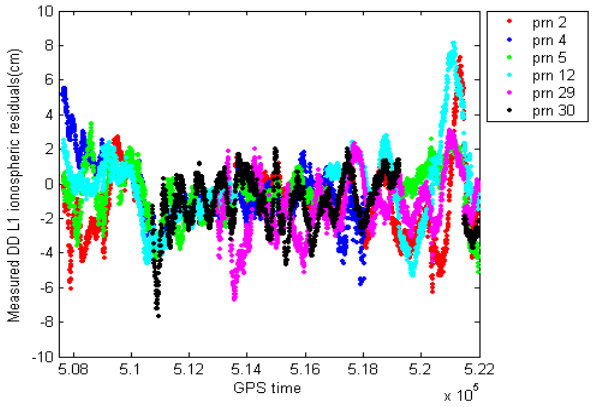

Figure 3b: Time series plots for the measured DD L1 ionospheric residuals of Baseline-B and six satellites, 4-hour data from Session B is used.

Table 3: RMS (cm) values for the measured DD L1 tropospheric and ionospheric residuals of Baseline-B and six satellites.

PRN	**2**	**4**	**5**	**12**	**29**	**30**
Trop.	2.5	2.7	2.8	1.7	5.2	4.1
Iono.	2.3	1.9	1.6	2.4	2.2	1.9

c) Baseline-C

Similarly, Figs 4a and 4b show the time series plots for the results of Baseline-C and six satellites. The test data from Session C is used. Table 4 shows the statistical values (RMS) for the results of the time series.

From Figs 4a and 4b, and Table 4, it can be seen:

1. The maximum values of the DD tropospheric and ionospheric residuals are about 9 cm and 12 cm respectively.
2. The RMS values of the DD tropospheric residuals are all less than that of the ionospheric residuals.

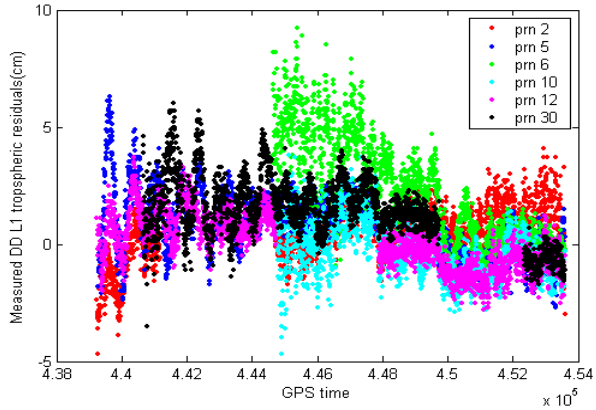

Figure 4a: Time series plots for the measured DD L1 tropospheric residuals of Baseline-C and six satellites, 4-hour data from Session C s used.

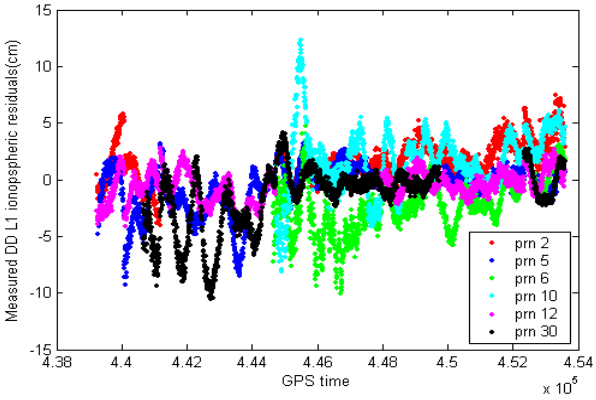

Figure 4b: Time series plots for the measured DD L1 ionospheric residuals of Baseline-C and six satellites, 4-hour data from Session C is used.

Table 4: RMS (cm) values for the measured DD L1 tropospheric and ionospheric residuals of Baseline-C and six satellites.

PRN	**2**	**5**	**6**	**10**	**12**	**30**
Trop.	1.3	1.6	3.1	1.2	1.2	2.0
Iono.	2.4	2.2	3.3	3.3	1.5	3.2

4.2 Temporal Variations

In this section, the temporal variation amplitudes of the tropospheric and ionospheric residuals in some fixed spans of short times and for the same satellite were compared. The test baselines and observation sessions are the same as that in Section 4.1 and the test results are presented as below.

a) Baseline-A

Figs 5a and 5b show the time series plots for the DD tropospheric and ionospheric residuals for PRNs 8 and 20 respectively. It should be noted that the broken periods in these graphs mean that during the time the satellites are taken as the reference satellites due to the

fact that their elevations are the highest (see the elevation plot).

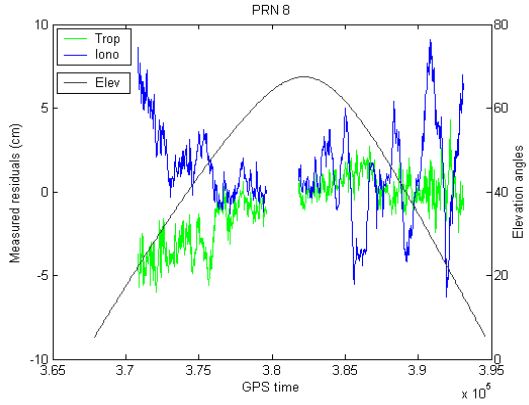

Figure 5a: Time series plots for the DD L1 tropospheric and ionospheric residuals of Baseline-A and PRN 8; data from Session A is used.

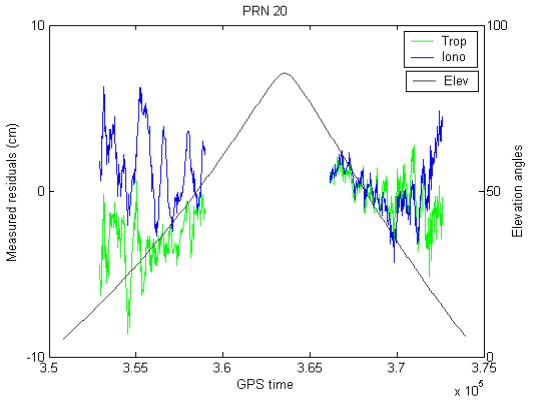

Figure 5b: Time series plots for the DD L1 tropospheric and ionospheric residuals of Baseline-A and PRN 20; data from Session A is used.

b) Baseline-B

Figs 6a and 6b show the test results for Baseline-B, and for PRNs 5 and 12 respectively.

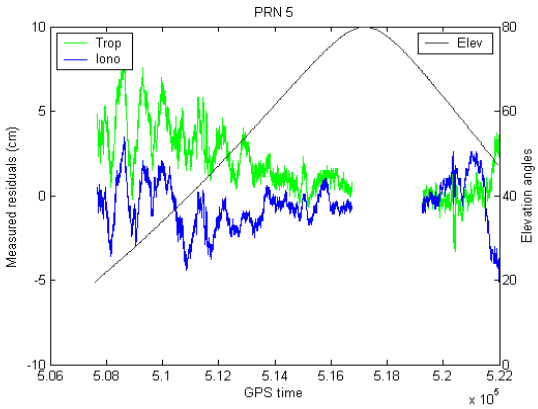

Figure 6a: Time series plots for the DD L1 tropospheric and ionospheric residuals for Baseline-B and PRN 5, the test data from Session B is used.

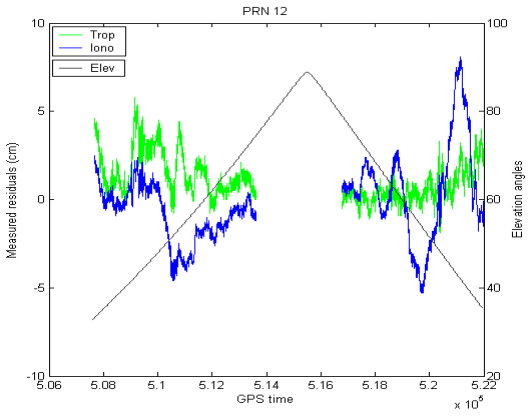

Figure 6b: Time series plots for the DD L1 tropospheric and ionospheric residuals of Baseline-B and PRN 12, data from Session B is used.

c) Baseline-C

Figs 7a and 7b show the test results for Baseline-C, and for PRNs 5 and 12 respectively.

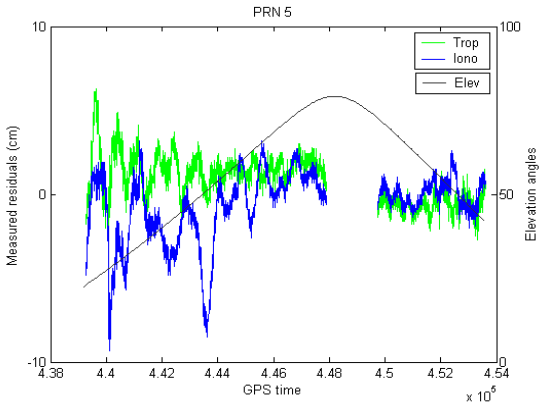

Figure 7a: Time series plots for the DD L1 tropospheric and ionospheric residuals of Baseline-C and PRN 5, data from Session C is used.

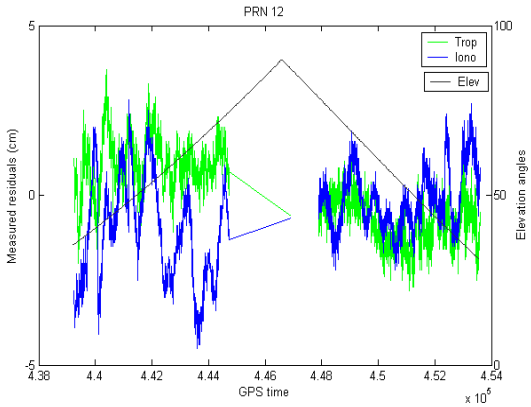

Figure 7b: Time series plots for the DD L1 tropospheric and ionospheric residuals of Baseline-C and PRN 12, data from Session C is used.

The differences in the values of the tropospheric (or ionospheric) residuals at any two epochs, e.g. two consecutive epochs or a few epochs of time spans indicate the temporal variation amplitudes of the tropospheric (or ionospheric) residuals. From Figs 5a−7b, the overall temporal variation amplitudes of the DD tropospheric and ionospheric residuals for the same time spans can be compared. From these figures, it can be found that for a span of a few epochs, the temporal variation amplitudes of the DD tropospheric residuals are not always significantly less than that of the ionospheric residuals. In many cases, both of them are quite similar and they can reach a level of several cm.

d) More Details for Trop.

For checking the temporal variation amplitudes of the tropospheric residuals more clearly, some plots for half an hour results with higher resolutions of time are shown in Figs 8a, 8b and 8c. The selected satellites in these three figures are PRNs 20, 5 and 12 respectively, which are the same as that in Figs 5b, 6a and 7b respectively. It should be noted that in these three figures, the X-axis denotes the time elapsed from the first epoch in the selected time slot rather than the real GPS observation time.

From Figs 8a, 8b and 8c, it can be seen that the temporal variation amplitudes of the DD tropospheric residuals can usually reach several cm in a one-minute time span. Fig. 8a shows that in a 30-second time span, these values can be more than 2 cm (see the difference of the values in the Y-axis at two consecutive data points). Figs 8a and 8b also show that within a three-minute time span, that value can reach 6 cm.

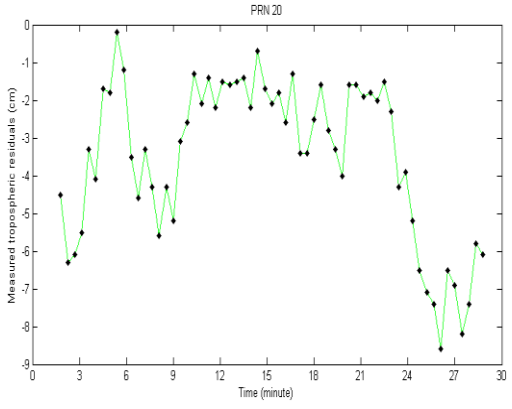

Fig. 8a Time series plots for the DD L1 tropospheric residuals of Baseline-A and PRN 20, test data is from Session A (the sampling rate is 30s).

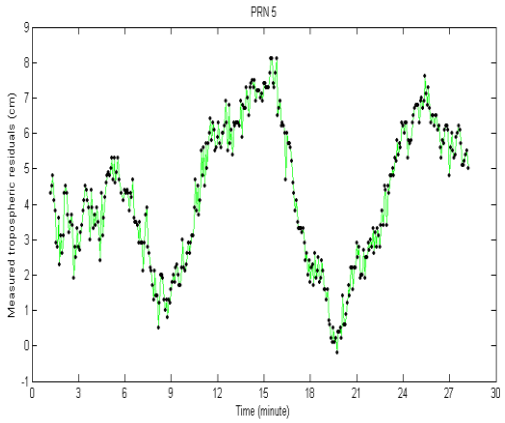

Fig. 8b Time series plots for the DD L1 tropospheric residuals of Baseline-B and PRN 5, test data is from Session B (the sampling rate is 5s).

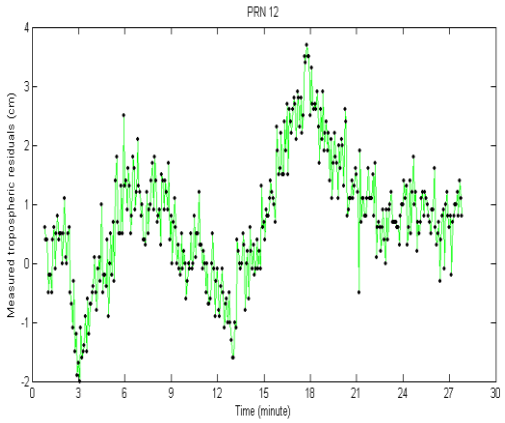

Fig, 8c Time series plots for the DD L1 tropospheric residuals of Baseline-C and PRN 12, test data is from Session C (the sampling rate is 5s).

The results from this section and the previous sections for the temporal variations of the DD tropospheric residuals suggest:

1. The DD tropospheric delays can significantly contaminate the DD GPS observations like the ionospheric delays do. Both types of the atmospheric errors should be treated equally important;
2. The temporal variation amplitudes of the DD tropospheric residuals within a fixed time span are not always significantly less than that of the ionospheric errors.

2) implies that the data generation and transmission for the DD tropospheric error corrections for the NRTK users shouldn't be less frequent than that for the ionospheric error corrections. This is because with a less-than-one-minute data latency, the tropospheric variations can reach a level of several cm. This may be an important instruction for the NRTK implementation of GPS*net*.

5. Conclusions

In this paper, comparisons for the magnitudes and temporal variation amplitudes of both DD tropospheric and ionospheric errors were conducted. The GPS data from three different observation sessions are used for the testing of the three baselines selected from four GPS*net* stations. The summary of the test results is:

1. The magnitudes of both DD tropospheric residuals and ionospheric errors were over 10 cm for the baseline lengths of 63-83 km. The both types of atmospheric effects on GPS observations were significant regardless of whether it was daytime and nighttime.
2. The temporal variation amplitudes of the DD tropospheric errors were not always significantly less than that of the ionospheric errors, and sometimes the former were greater than the latter. These values for the tropospheric errors sometimes could reach several cm in a one-minute time span and 2 cm in a 30-second time span respectively.

The implications of these results are that the DD tropospheric errors should be taken and treated as seriously as for the ionospheric errors in the implementation of the NRTK. For example, the generation and transmission of the corrections for the tropospheric errors should not be significantly less frequent than that for the ionospheric corrections, like implied by some researchers. The DD atmospheric errors derived from four one-way observations are more related to the geometry of the associated two satellites and two receivers.

Acknowledgments

The author would like to gratefully acknowledge the research fund granted for this project through the Australian Research Council (LP0455170).

References

Chen, X., Han, S., Rizos, C. and Goh, P. C. (2000) ***Improving real-time positioning efficiency using the Singapore Integrated Multiple Reference Station Network (SIMRSN).*** 13th Int. Tech. Meeting of the Satellite Division of the U.S. Inst. of Navigation, Salt Lake City, Utah, USA, Sept. 19−22, 9−18.

Hofmann-Wellenhof, B., Lichtenegger, H. and Collins, J. (1997) ***Global Positioning System: Theory and Practice***. (Fourth Edition edition), Springer-Verlag, Berlin.

IGSCB (2009) ***IGS Product.*** Retrieved Mar. 13, 2009, from http://igscb.jpl.nasa.gov/components/prods.html

SII (2008) ***Vicmap position -GPSnet.*** Retrieved Jun. 20, 2008, from http://www.land.vic.gov.au.

Wu, S. (2009) ***Performance of Regional Atmospheric Error Models for NRTK in GPSnet and the Implementation of A NRTK System***. Ph.D Thesis, School of Mathematical and Geospatial Sciences, RMIT University, Melbourne, Australia.

Biography

Dr Suqin Wu is currently a research fellow at the School of Mathematical and Geospatial Sciences, RMIT University, Australia. She received her PhD from the same school and university in 2009. Her current research involves algorithms and implementation for high accuracy, real-time GPS positioning based on multiple reference station networks. She also conducts research related to the algorithms and performance of precise orbit determination and radio occultation technique for atmospheric parameter profiles.